LETTERS

Room-Temperature Fluorescence Imaging and Spectroscopy of Single Molecules by Two-Photon Excitation

Erik J. Sánchez,[†] Lukas Novotny, Gary R. Holtom, and X. Sunney Xie*,[†]

Pacific Northwest National Laboratory, Environmental Molecular Sciences Laboratory, P.O. Box 999, Richland, Washington 99352

Received: June 11, 1997; In Final Form: July 22, 1997[⊗]

We report fluorescence imaging of single dye molecules on a glass substrate by two-photon excitation with femtosecond pulses from a mode-locked Ti:sapphire laser. The single-molecule images exhibit a high signal to background ratio ($>30:1$) and a high spatial resolution (fwhm $< \lambda/3$). A quadratic intensity dependence of single-molecule emission rate is experimentally verified, and single-molecule emission spectra are recorded with two-photon excitation. A comparison of photobleaching rates is made between one-photon and two-photon excitation schemes.

Introduction

Recently two-photon fluorescence microscopy has become a powerful tool for high-resolution three-dimensional imaging of biological systems.[1] In contrast to conventional confocal microscopy with one-photon excitation, two-photon excitation results in a small excitation volume, allowing the minimization of photodamage of the sample and the discrimination of background signals. It also permits a deeper penetration depth for thick biological samples.

There have been tremendous developments in recent years of detection, imaging and spectroscopy of single molecules. With one-photon fluorescence excitation, detection of single molecules in solution,[2-6] imaging of immobilized molecules at interfaces[7,8] and in solids[9] with near-field and far-field microscopy, and imaging of a field of moving molecules with a CCD camera[10-12] have been demonstrated. The high sensitivity of the imaging techniques allowed the extension of spectroscopic work done at cryogenic temperature[13] to the room-temperature regime.[14,15] Fluorescence lifetime measurements[16-19] allowed

probing excited state dynamics of single molecules. All these advances have resulted in a paradigm for studying many single-molecule behaviors, e.g. translational[10,12,20] and rotational diffusion,[21] spectral diffusion,[22,23] energy transfer,[24,19] electron transfer,[25] and enzymatic reactions.[11,26-28] Many of these single-molecule experiments have begun to offer detailed information regarding molecular interaction and dynamics that are otherwise difficult to obtain from ensemble-averaged results of heterogeneous systems, in particular, biological systems.

In principle, most of these single-molecule experiments could be done with two-photon excitation if the advantages of the two-photon excitation are desired. With two-photon excitation, detection of single rhodamine B (RhB) molecules in a dilute methanol solution has been recently demonstrated by Xu and Webb.[29] Plakhotnik et al. have demonstrated high frequency resolution two-photon spectroscopy of single molecules at cryogenic temperatures.[30] In this Letter, we report fluorescence imaging and spectroscopy of single immobilized molecules with two-photon excitation in an ambient environment. The signal to background ratio and the spatial resolution are compared to those of one-photon excitation. We also compare the photobleaching lifetimes in the one- and two-photon excitations and

---

* Author to whom the correspondence should be addressed.

† Also affiliated with Physics Department, Portland State University.

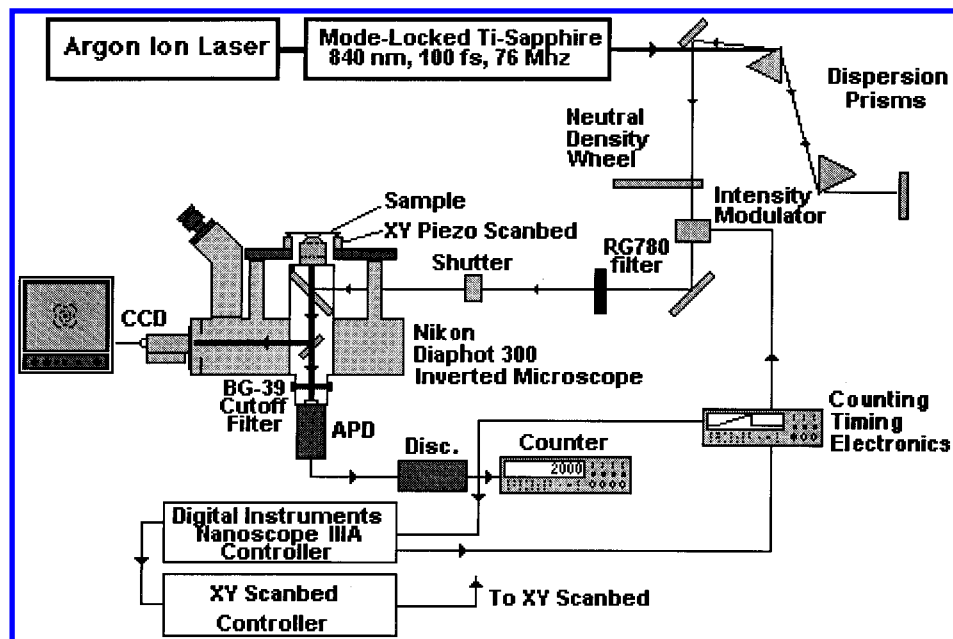⊗ Abstract published in *Advance ACS Abstracts,* September 1, 1997.

Figure 1. Schematic of the combination of the mode-locked Ti-sapphire laser, the inverted fluorescence microscope, and the detection system.

discuss the photophysics associated with the differences. This information will be useful for future studies with two-photon microscopy and spectroscopy.

Experimental Section

The schematic of our apparatus is shown in Figure 1. The light source for two-photon excitation is a mode-locked Ti-sapphire laser (Coherent Mira 900) providing 100 fs pulses at a repetition rate of 76 MHz and tunable from 790 to 900 nm. The beam was sent into an inverted fluorescence microscope (Nikon Diaphot 300) and was reflected by a dichroic beam splitter (Chroma #725DCSP) into a microscope objective (Nikon Apochromatic, 60×, 1.4 NA). An SF11 prism pair is used to precompensate the group velocity dispersion in the objective lens so that the pulse widths at the sample are approximately 180 fs. The average excitation power was 0.2−3 mW at the diffraction-limited focal spot.

Fluorescence was collected by the same objective lens, filtered by the combination of the dichroic filter and a Schott BG39 filter, and detected by a photon-counting avalanche photodiode (APD) (EG&G SPCM 200). The use of a BG-39 Schott glass filter allows the passage of essential the whole visible light spectrum with good transmission. Different fluorescent molecules can be used without changing the filters. At a high excitation power (>2 mW), we also observed second harmonic generation at the sample surface and a broad band emission not from the molecules, which exhibits a quadratic intensity dependence. However, these signals can be suppressed by other filters.

The sample was mounted on a 50×50 μm^2 closed loop scan bed (Physik Instrumente). A modified Nanoscope IIIA controller (Digital Instruments) was used for controlling the scan bed and image acquisition. An image is composed of 256×256 pixels with a line scan rate of 1 Hz. After an image is obtained, a particular immobilized molecule can be placed onto the focus so that measurements can be made before it is photobleached. Sample preparation was done by making a methanol solution of 10^{-9} M dye and spin coating 20 μL at 5000 rpm onto cover glass slides (Fisher Scientific 22 CIR-1). All measurements were done under ambient conditions.

Results and Discussion

Figure 2 shows a 5 μm $\times$ 5 μm fluorescence image of single RhB molecules on a glass substrate taken with the apparatus described above. Similar images have been obtained for many other molecules, including Coumarin 535 and DCM. In recording the image in Figure 2, the wavelength of the laser was tuned to 840 nm, where the maximum of the two-photon absorption cross section of RhB molecules was observed.[31] Each peak in Figure 2 is due to a single molecule, evidenced by the abrupt disappearance of the signal in the subsequent images as the result of photobleaching, and the linearly polarized fluorescence expected from a single emitting dipole. The variation in intensities of the molecules are due to different molecular orientations and absorption spectra. The signal to background ratio is 30:1, which is comparable to many fluorescence images of single molecules with one-photon excitation. It is noteworthy that full-width at half-maxima (fwhm) of the peaks are around 250 nm ($<^{\lambda}/_3$), significantly smaller than is the case for one-photon excitation. This narrower point spread function is the result of the quadratic intensity dependence of the two-photon excitation.

Below saturation, the fluorescence count rate (photon/s) from a single molecule is expected to be[1]

$$C_f \propto \frac{qK\sigma^{(2)}N_A^4\langle P\rangle^2}{\lambda^2\tau f} \tag{1}$$

where q is the fluorescence quantum efficiency, K is the fluorescence detection efficiency; $\sigma^{(2)}$ is the two-photon absorption cross section (in units of (m^4 s/photon), N_A is the numerical aperture of the objective lens, $\langle P\rangle$ is the average excitation power (in W) at the sample; λ is the center wavelength of the light pulses; f is the repetition rate of the pulse train, and τ is the pulse width.

Indeed a quadratic intensity dependence is observed for the single-molecule emission, while the background signal shows a linear intensity dependence. Figure 3 shows the log−log plot of C_f versus $\langle P\rangle$ measured on a single RhB molecule. The slope of the fitted line is 1.98. All the molecules examined show slopes close to 2. This proves that the emission signal is from two-photon excitations of single molecules and the saturation is not reached at average power levels under 3 mW.
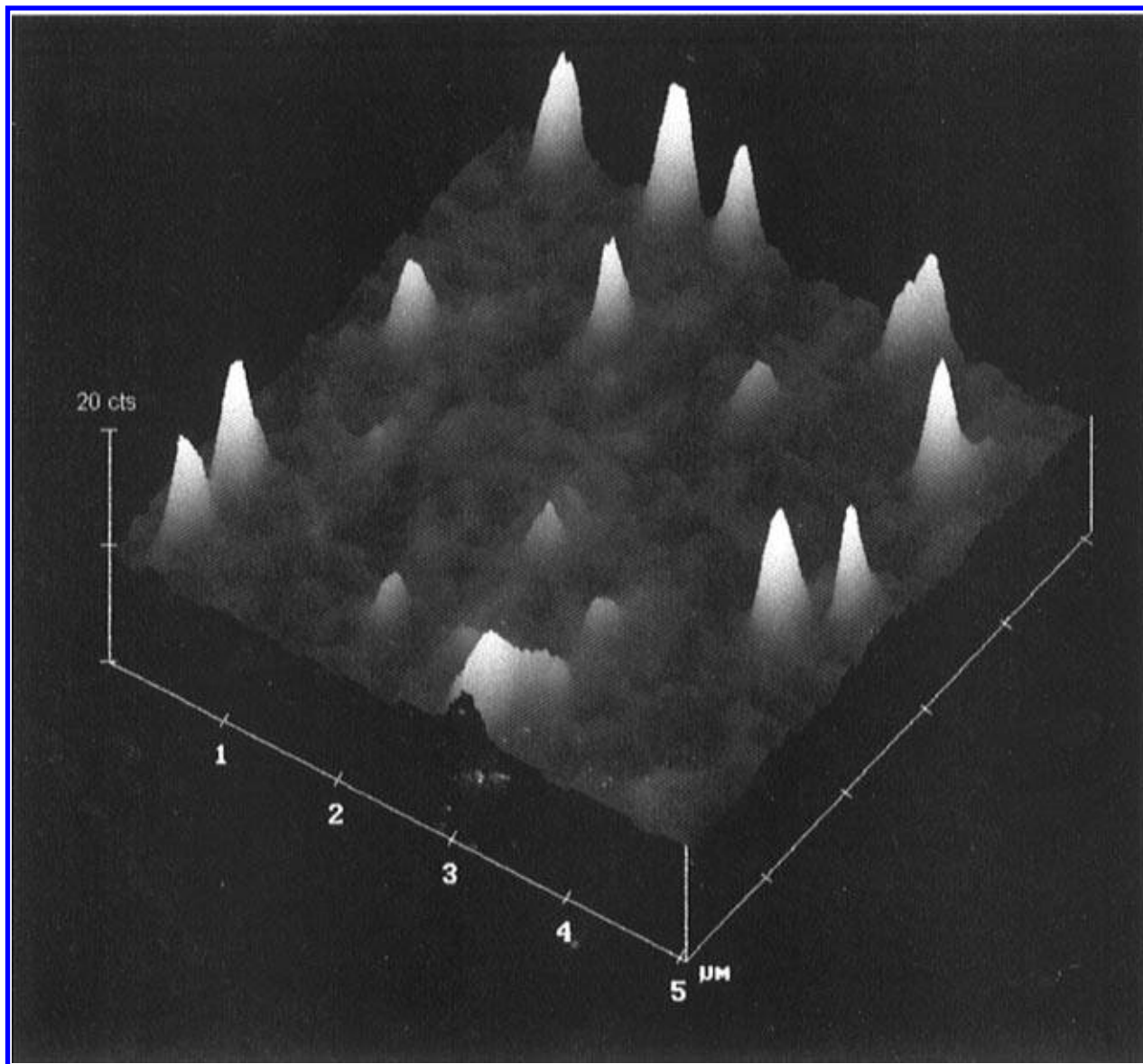
Letters

J. Phys. Chem. A, Vol. 101, No. 38, 1997 **7021**

Figure 2. Fluorescence image of single immobilized RhB dye molecules in a 5 μm $\times$ 5 μm field taken with two-photon excitation (5 min acquisition time). Each peak was due to a single molecule with the fwhm being 250 nm ($<^{\lambda}/_3$), smaller than is the case for one-photon excitation due to the quadratic intensity dependence. The molecules are dispersed on a glass substrate. The femtosecond pulse train at the sample had an average power of 400 μW, center wavelength of 840 nm, and pulse width of 180 fs.

In determining the count rate dependence shown in Figure 3, we first attempted to create a linear ramp of the excitation power on single molecules and to determine the count rate by accumulating emission counts in fixed time bins. However, this scheme is problematic: at low power levels, fewer emission counts result in poor signal to noise ratio. On the other hand, at high power levels, high emission rates result in fast photo-bleaching. Furthermore, it has been established in one-photon excitation experiments that there are photoinduced fluctuations in emission intensity of single immobilized molecules,[23] which resulted in additional variations at the higher power levels.

In order to avoid the fast photobeaching and to minimize the photoinduced artifacts, equally distributed emission counts over the entire range of data points is desired. In recording the data in Figure 3, the molecule was held at a certain power level until a specific number of photon counts (100) was reached; the power level was then adjusted to the next value. While the number of photons was fixed at each data point, the time needed to reach the preset number was measured. C_f is the count/time ratio. In practice, a liquid crystal laser intensity modulator

(ThorLab) in the laser beam was used to electrooptically adjust the excitation power. The modulator kept the excitation power constant at a level set by the computer during each acquisition of C_f. The power level was then advanced to the next value before the counting and timing electronics started again. The maximum laser power throughput of the liquid crystal restricts our ability to reach the saturation levels on individual molecules. However other electrooptical modulators can be used for higher powers.

Once a single molecule is located in a fluorescence image, its emission spectrum can be recorded with a combination of a back-illuminated CCD camera (Princeton Instruments, LN/CCD-512TKB/1) and a spectrograph (Acton 150). Figure 4 shows the emission spectra for an individual RhB molecule. The average excitation power level was 400 μW at 840 nm. The exposure time of the CCD was 2 s; the fluorescence for this particular single molecule stopped after $\sim$3 s. The emission spectrum of identical molecules in different locations showed a large spectral inhomogeneity, consistent with the observations made with one-photon excitation.[8,23] However, there is no
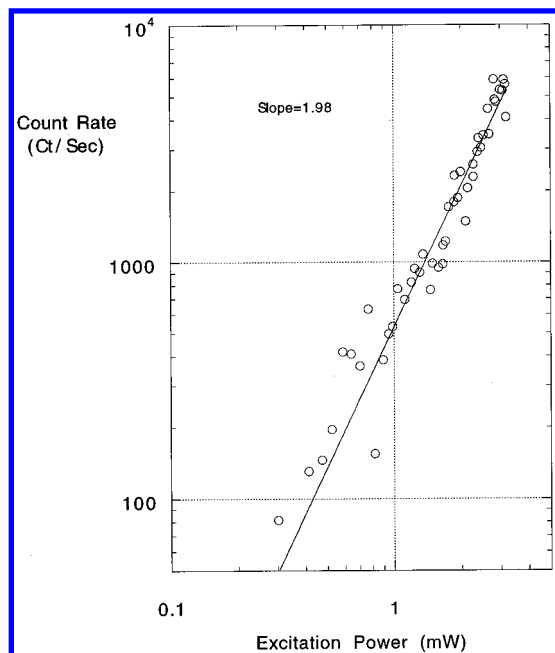
Figure 3. Log−log plot of the count rate (C_f) of a single RhB molecule as a function of the averaged two-photon excitation power ($\langle P \rangle$) at 840 nm. The slope of the fitted line is 1.98, proving the quadratic dependence on the excitation power for the single-molecule emission. The power range of 0.2−3 mW was below saturation.
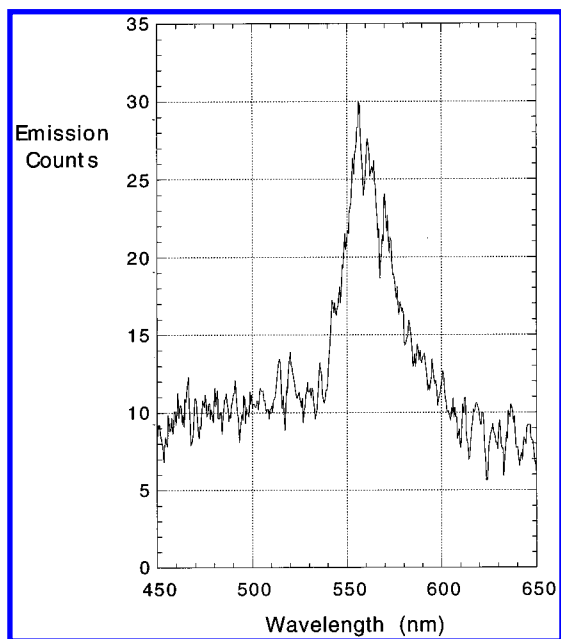

Figure 4. Room-temperature emission spectrum of a single RhB molecule obtained by two-photon excitation. There is no evidence that emission spectra with two-photon excitation are different from those with one-photon excitation.

evidence that emission spectra obtained with two-photon excitation is different from those obtained with one-photon excitation.

Next, we make a comparison of the photobleaching lifetimes, defined as the total number of emitted photons before photobleaching, for one and two-photon excitation. This was done on RhB molecules deposited onto glass substrates. The one-photon excitation was with 1 μW CW light at 532 nm from a frequency-doubled diode-pumped Nd:YAG Laser (Sante Fe Laser), and the two-photon excitation was as described above with an average excitation power of 490 μW. The collection efficiency of the entire detection system (K) was carefully optimized and determined to be close to 0.1 for both one-photon
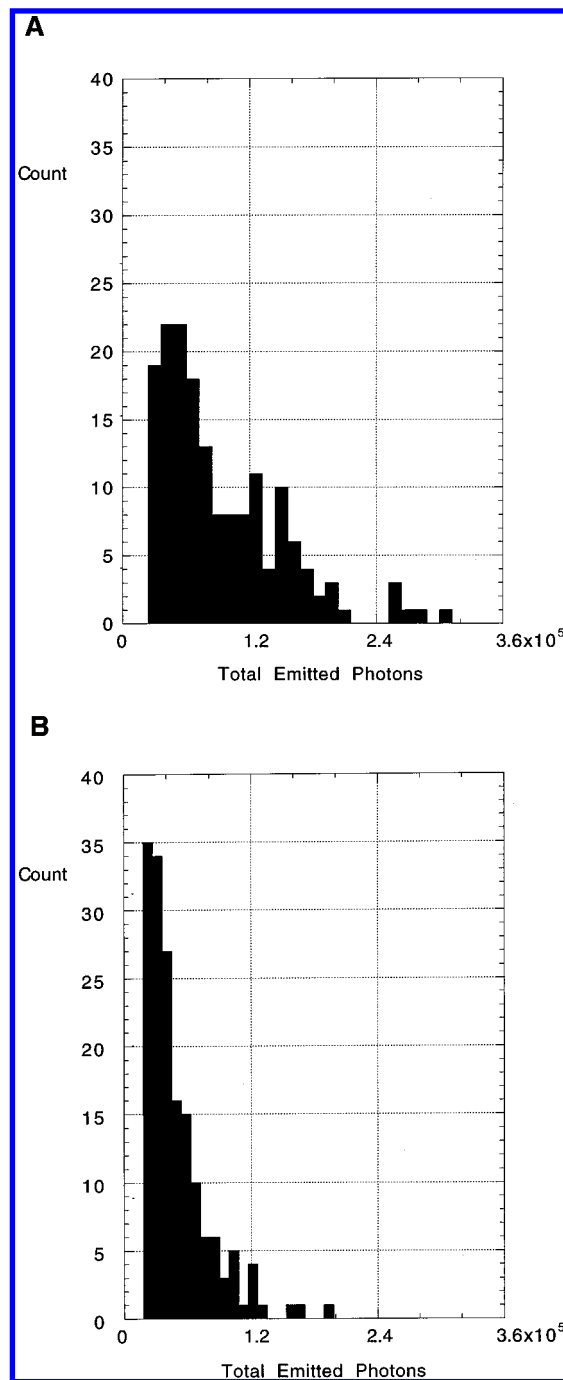

Figure 5. (A) Histogram of total emitted photons before photobleaching, derived from 165 single RhB molecules subject to one-photon CW excitation at 532 nm. (B) Histogram of 165 single RhB molecules subject to two-photon excitation with femtosecond pulses at 840 nm.

and two-photon excitation experiments (different dichroic and color filters). In both cases, linear polarization of excitation was used. Despite the fact that different molecular orientations or absorption spectra resulted in different emission rates, only the total number of emitted photons prior to photobleaching was counted. This was done by taking as many 10 × 10 μm^2 fluorescence images as necessary until all molecules photobleached. All recorded frames were then added together. The scan bed had no drift during data accumulation, so that all frames coincided with each other when superimposed.

Parts A and B of Figure 5 show the histograms for the photobleaching lifetimes for one-photon and two-photon excitation, respectively. Each histogram was constructed from 165 single RhB molecules. Both histograms exhibit exponential

Letters

J. Phys. Chem. A, Vol. 101, No. 38, 1997 **7023**

distributions with the lifetime for one-photon excitation being roughly twice as long as for two-photon excitation. The mean lifetimes are 18 500 and 8 500 counts for one and two-photon excitation, respectively. It is interesting to note that on a single-molecule basis, two-photon excitation actually accelerates photobleaching, even though the two-photon imaging in a thick tissue is expected to reduce photobleaching because of the reduced excitation volume. However, we caution that this phenomena could depend on the molecule and the wavelength.

Photochemistry and photophysics of xanthene (rhodamine) dyes have been extensively studied.[32] Photobleaching of xanthene dyes often results from multiphoton processes. In particular, a mechanism proposed involves triplet absorption to a upper triplet state (eq 2), which is sufficiently energetic to abstract hydrogen from alcohol solvent to produce the radicals observed by electron spin resonance.[33]

$$S_0 \xrightarrow{h\nu} S_1 \rightarrow T_1 \xrightarrow{h\nu} T_n \rightarrow H \text{ abstraction} \qquad (2)$$
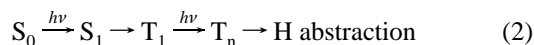
The $T_1 \rightarrow T_n$ absorption band is lower in energy and broader in width than the $S_0 \rightarrow S_1$ absorption band, in resonance with the 840 nm excitation light. Once a T_1 state is reached through the repetitive excitation of a single molecule, the femtosecond light can be absorbed or even saturate the $T_1 \rightarrow T_n$ transition during the long triplet lifetimes (10 μs to 10 ms), resulting in the hydrogen abstraction from residual methanol or the water layer on the surface, or other photochemical reactions. This may explain the faster photobleaching rate associated with the two-photon excitation. Other photobleaching mechanisms such as those involving singlet oxygen[34] are also possible. While many events of photobleaching were irreversible, we also observed that some molecules, apparently irreversibly photobleached, reappeared after being in the dark for several hours. The reversible photobleaching indicates a reversible photochemical reaction.

Conclusion

In summary, we demonstrate the capability to image fluorescence from single molecules at room temperature by two-photon excitation with femtosecond pulses. In addition to the effective background rejection and the improved spatial resolution, the high sensitivity of the two-photon scheme allows two-photon spectroscopic measurements on single molecules at a moderate excitation power well below saturation. For immobilized RhB molecules, the photobleaching rates for two-photon excitation are determined to be twice as fast as for one-photon excitation.

References and Notes

(1) For a review, see: Denk, Winfried; Piston, David W.; Webb, Watt W. *Handbook of Biological Confocal Microscopy*; Plenum Press: New York, 1995, pp 445−458.

(2) Keller, R. A.; Ambrose, W. P.; Goodwin, P. M.; Jett, J. H.; Martin, J. C.; Wu, M. *Appl. Spectrosc.* **1996**, *50*, 12A.

(3) Eigen, M.; Rigler, R. *Proc. Natl. Acad. Sci. U.S.A.* **1994**, *91*, 5740.

(4) Nie, S.; Chiu, D. T.; Zare, R. N. *Science* **1994**, *266*, 1018.

(5) Haab, B. B.; Mathies, R. A. *Anal. Chem.* **1995**, 67, 3235.

(6) Barnes, M. D.; Whitten, W. B.; Ramsey, J. M. *Anal. Chem.* **1995**, *67,* 418A.

(7) Betzig, E.; Chichester, R. J. *Science* **1993**, *262*, 1422.

(8) Macklin, J. J.; Trautman, J. K.; Harris, T. D.; Brus, L. E. *Science* **1996**, *272*, 255.

(9) Gutther, F.; Irngartinger, T.; Traber, M.; Renn, A.; Wild, U. P. *Rev. Sci. Instrum.* **1996**, *67*, 1425.

(10) Schmidt, Th.; Schutz, G. J.; Baumgartner, W.; Gruber, H. J.; Schindler, H. *J. Phys. Chem.* **1995**, *99*, 17662.

(11) Funatsu, T.; Harada, Y.; Tokunaga, M.; Saito, K.; Yanagida, T. *Nature* **1995**, *374*, 555.

(12) Dickson, R. A.; Norris, D. J.; Tzeng, Y.; Moerner, W. E. *Science* **1996**, *274*, 966

(13) For a review, see: *Single-molecule Optical Detection, Imaging and Spectroscopy;* Basche, T., Moerner, W. E., Orrit, M., Wild, U. P., Eds.; VCH: New York, 1997.

(14) For a review, see: Xie, X. S. *Acc. Chem. Res*. **1996**, *29*, 598.

(15) For a review, see: Trautman, J. K.; Ambrose, W. P. In ref 13.

(16) Xie, X. S.; Dunn, R. C. *Science* **1994**, *265*, 361.

(17) Ambrose, W. P.; Goodwin, P. M.; Martin, J. C.; Keller, R. A. *Science* **1994**, *265*, 364.

(18) Trautman, J. K.; Macklin, J. J. *Chem Phys.* **1996**, *205*, 221.

(19) Bian, R. X.; Dunn, R. C.; Xie, X. S.; Leung, P. T. *Phys. Rev. Lett.* **1995**, *75*, 4772.

(20) Bopp, M. A.; Meixner, A. J.; Tarrach, G.; Zschokke-Granacher, I.; Novotny, L. *Chem. Phys. Lett.* **1996**, *263*, 721.

(21) Ha, T.; Enderle, T.; Chemla, D. S.; Selvin, P. R.; Weiss, S. *Phys. Rev. Lett.* **1996**, *77*, 3979.

(22) Trautman, J. K.; Macklin, J. J.; Brus, L. E.; Betzig, E. *Nature* **1994**, *369*, 40.

(23) Lu, H. P.; Xie, X. S. *Nature* **1997***, 385,* 143.

(24) Ha, T.; Enderle, Th.; Ogletree, D. F.; Chemla, D. S.; Selvin, P.; Weiss, S. *Proc. Natl. Acad. Sci. U.S.A.* **1996**, *93*, 624.

(25) Lu, H. P.; Xie, X. S. *J. Phys. Chem.* **1997***, 101*, 2753.

(26) Xue, Q. F.; Yeung, E. S. *Nature* **1995**, *373*, 681.

(27) Craig, D. B.; Arriaga, E. A.; Wong, J. C. Y.; Lu, H.; Dovichi, N. J. *J. Am. Chem. Soc.* **1996**, *118*, 5245.

(28) Vale, R. D.; Funatsu, T.; Pierce, D. W.; Romberg, L.; Harada Y.; Yanagida, T. *Nature* **1996**, *380*, 451.

(29) Mertz, J.; Xu, C.; Webb, W. W. *Opt. Lett.* **1995**, *20*, 2532.

(30) Plakhotnik, T.;Walser, D.; Pirotta, M.; Renn, A.; Wild, U. P. *Science* **1996**, *271*, 1703.

(31) Xu, C.; Webb, W. W. *J. Opt. Soc. Am. B.* **1996**, *12*, 481.

(32) For a review, see: Jones, G., II. In *Dye Laser Principles*; Duarte, F. J., Hillman, L. W., Eds.; Academic Press: New York, 1990.

(33) Yamashita, M.; Kashiwagi, H. *IEEE J. Quantum. Electr*on. **1976**, *QE-12*, 90−95.

(34) For a review, see: Foot, C. S.; Clennan, E. L. In *Active Oxygen in Chemistry*; Foote, C. S., Valentine, J. S., Greenberg, A., Liebman, J. F., Eds.; Blackie Academic & Professional: London, 1995; p 105.